

SPG Mitteilungen Communications de la SSP

Auszug - Extrait

The first image of a black hole

PT 3/2021

Luciano Rezzolla ^{1,2,3} and The Event Horizon Telescope Collaboration

¹ Institut für Theoretische Physik, Max-von-Laue-Straße 1, 60438 Frankfurt am Main, Germany

² Frankfurt Institute for Advanced Studies, Ruth-Moufang-Str. 1, 60438 Frankfurt am Main, Germany

³ School of Mathematics, Trinity College, Dublin 2, Ireland

This article has been downloaded from:

https://www.sps.ch/fileadmin/articles-pdf/2021/Mitteilungen_PT032021.pdf

© see https://www.sps.ch/bottom_menu/impressum/

The first image of a black hole

PT 3/2021

Luciano Rezzolla^{1,2,3} and The Event Horizon Telescope Collaboration

¹ Institut für Theoretische Physik, Max-von-Laue-Straße 1, 60438 Frankfurt am Main, Germany

² Frankfurt Institute for Advanced Studies, Ruth-Moufang-Str. 1, 60438 Frankfurt am Main, Germany

³ School of Mathematics, Trinity College, Dublin 2, Ireland

When surrounded by a transparent emission region, black holes are expected to reveal a dark shadow caused by gravitational light bending and photon capture at the event horizon. To image and study this phenomenon, in April 2019, the Event Horizon Telescope (EHT) Collaboration reported the first observations of a global very long baseline interferometry (VLBI) array observing at a wavelength of 1.3 mm. These observations have allowed us to reconstruct event-horizon-scale images of the supermassive black hole candidate in the center of the giant elliptical galaxy M87.

We have resolved the central compact radio source as an asymmetric bright emission ring with a diameter of $42 \pm 3 \mu\text{as}$, which is circular and encompasses a central depression in brightness with a flux ratio $\geq 10 : 1$ (see Fig. 1). The emission ring is recovered using different calibration and imaging schemes, with its diameter and width remaining stable over four different observations carried out in different days. Overall, the observed image is consistent with expectations for the shadow of a Kerr black hole as predicted by general relativity. The asymmetry in brightness in the ring can be explained in terms of relativistic beaming of the emission from a plasma rotating close to the speed of light around a black hole. By comparing the EHT observed images to an extensive library of ray-traced general-relativistic magnetohydrodynamic (GRMHD) simulations of black holes, it was possible to derive a central mass of $M = (6.5 \pm 0.7) \times 10^9 M_{\odot}$.

While the capability of the Event Horizon Telescope (EHT) to image the nearest supermassive black hole candidates at horizon-scale resolutions offers a novel means to study gravity in its strongest regimes and to test different models for these objects, it is not always simple to rule out alternatives to black holes in general relativity. Indeed, while the Kerr metric remains a solution in some alternative theories of gravity, non-Kerr black hole solutions do exist in a variety of such modified theories. This is because a shadow can be produced by any compact object with a spacetime characterized by unstable circular photon orbits [2]. Furthermore, exotic alternatives to black holes, such as naked singularities [3] and gravastars [4, 5], are admissible solutions within general relativity and provide concrete, albeit contrived, models. Some of such exotic compact objects can already be shown to be incompatible with our observations given our maximum mass prior. For example, the shadows of naked singularities associated with Kerr spacetimes with $|a_{*}| > 1$ are substantially smaller and very asymmetric compared to those of Kerr black holes [6].

In order to assess our present ability to use EHT images to determine if they correspond to a Kerr black hole as predicted by Einstein's theory of general relativity or to a black hole in alternative theories of gravity. To this end, we have performed (GRMHD) simulations and use general-relativistic radiative transfer (GRRT) calculations to generate synthetic shadow images of a magnetised accretion flow onto a Kerr black hole. In addition, and for the first time, we have

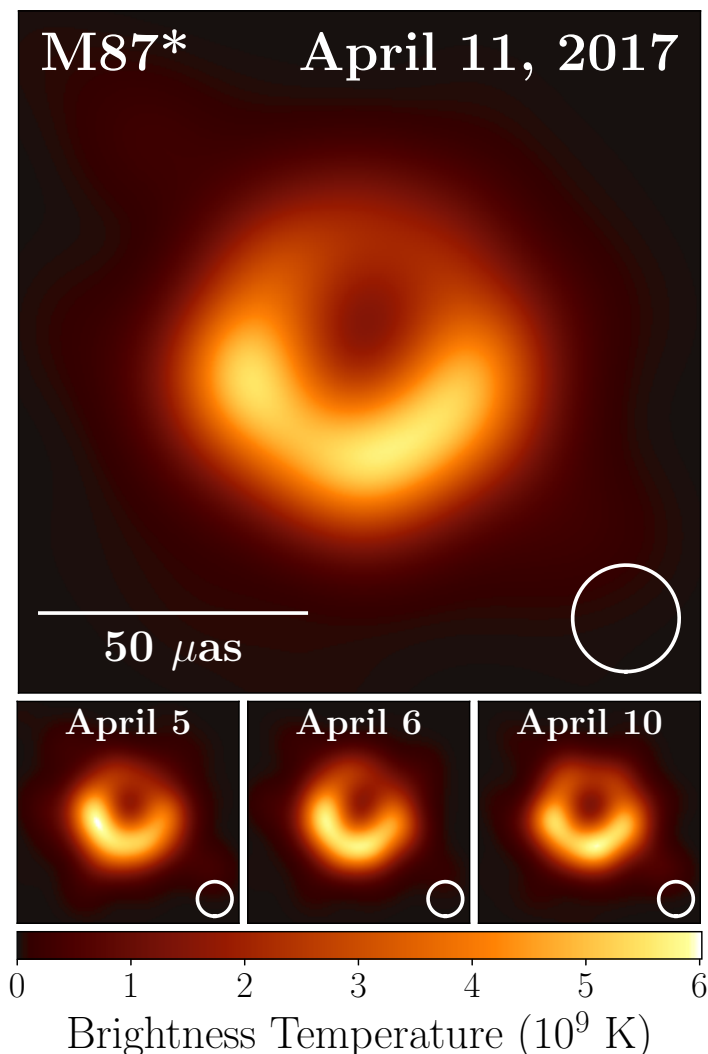


FIG. 1. Top: EHT image of M87* from observations on April 11, 2017 as a representative example of the images collected in the 2017 campaign. The image is the average of three different imaging methods after convolving each with a circular Gaussian kernel to give matched resolutions. The largest of the three kernels ($20 \mu\text{as}$ FWHM) is shown in the lower right. The image is shown in units of brightness temperature, $T_b = S\lambda^2/2k_B\Omega$, where S is the flux density, λ is the observing wavelength, k_B is the Boltzmann constant, and Ω is the solid angle of the resolution element. Bottom: Similar images taken over different days showing the stability of the basic image structure and the equivalence among different days.

performed GRMHD simulations and GRRT calculations for a dilaton black hole, which we take as a representative solution of an alternative theory of gravity. Adopting the VLBI configuration from the 2017 EHTC campaign, we find that it could be extremely difficult to distinguish between black holes from different theories of gravity [2] (see Fig. 2). These results highlight that great caution is needed when interpreting black hole images as tests of general relativity.

Finally, when interpreting the EHT images it can be instructive to other compact-object candidates – such as boson stars – which possess an unstable circular photon orbit but

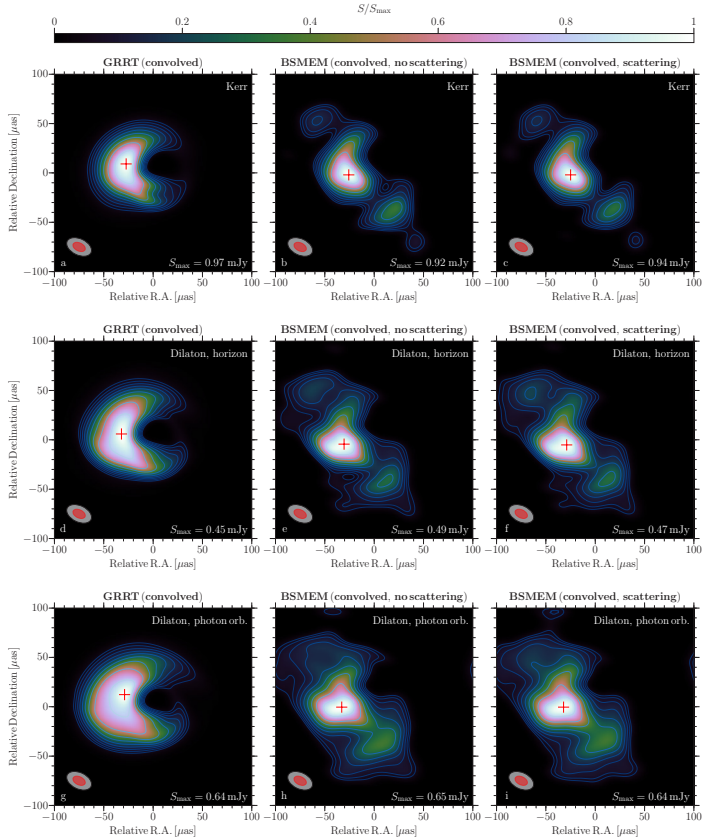


FIG. 2. Synthetic BH shadow images of Sgr A* for the Kerr BH using two different image reconstruction algorithms. From left to right: GRRT image convolved with 50% (red shading) of the nominal beam size (light grey shading), the contour levels start at 5% of the peak value and increase by $\sqrt{2}$. The red cross in the images marks the position of the flux density maximum (panel a), reconstructed image without interstellar scattering convolved with 50% (red shading) of the nominal beam size (light grey shading, panel b), and reconstructed image without interstellar scattering using BSMEM (panel c). All images are based on visibilities which take into account a possible VLBI antenna configuration and schedule for the EHTC April 2017 observations. The convolving beam is plotted in the lower left corner of each panel (see Ref. [2] for details).

are without a surface or an event horizon [7, 8]. In such spacetimes, null geodesics are redirected outwards towards distant observers [9], so that the shadow can in principle be filled with emission from lensed images of distant radio sources generating a complex mirror image of the sky.

Also in this case, we have performed GRMHD simulations of accretion flows in the boson-star spacetime, followed by GRRT calculations. The synthetic reconstructed images considering realistic astronomical observing conditions show that, despite qualitative similarities, the differences in the appearance of a black hole – either rotating or not – and a boson star are large enough to be detectable [10] (see Fig. 3). The origin of this difference is to be found in the fact that accretion flows onto boson stars behave differently from the corresponding flows onto black holes. These differences arise from dynamical effects directly related to the absence of an event horizon, in particular, the accumulation of matter in the form of a small torus or a spheroidal cloud in the interior of the boson star, and the absence of an evac-

uated high-magnetisation funnel in the polar regions. The mechanism behind these effects is general enough to apply to other horizonless and surfaceless black hole mimickers, strengthening confidence in the ability of the EHT to identify such objects via radio observations.

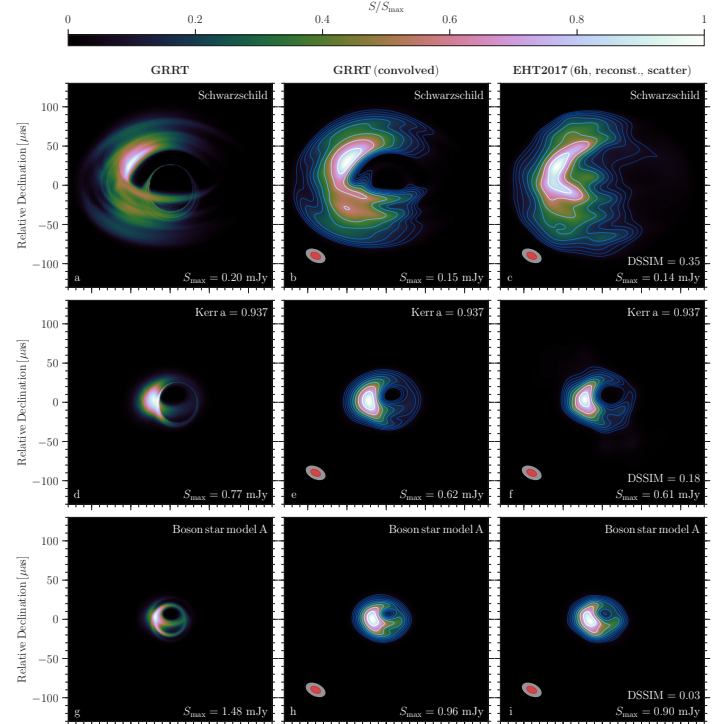


FIG. 3. From top to bottom: ray-traced and synthetic images at 230 GHz and inclination angle of $\theta_{\text{obs}} = 60^\circ$ of the Schwarzschild black hole (first row), the Kerr black hole (second row), and boson-star models A (third row). From left to right, first column: ray-traced images averaged over the interval $t/M \in [8900, 10000]$, second column: ray-traced images convolved with 50% (red shaded ellipse) of the EHTC beam (grey shaded ellipse), third column: reconstructed images including interstellar scattering, convolved with 50% (red shaded ellipse) of the EHTC beam (grey shaded ellipse) and indicating the value of the DSSIM metric (see Ref. [10] for details).

- [1] D. Psaltis, Living Rev. Relativ. **11**, 9 (2008), arXiv:0806.1531.
- [2] Y. Mizuno, Z. Younsi, C. M. Fromm, O. Porth, M. De Laurentis, H. Olivares, H. Falcke, M. Kramer, and L. Rezzolla, Nature Astronomy **2**, 585 (2018), arXiv:1804.05812 [astro-ph.GA].
- [3] R. Shaikh, P. Kocherlakota, R. Narayan, and P. S. Joshi, Mon. Not. R. Astron. Soc. **482**, 52 (2019), arXiv:1802.08060 [astro-ph.HE].
- [4] P. O. Mazur and E. Mottola, Proc. Nat. Acad. Sci. **101**, 9545 (2004), gr-qc/0407075.
- [5] C. B. M. H. Chirenti and L. Rezzolla, Class. Quantum Grav. **24**, 4191 (2007), arXiv:0706.1513 [gr-qc].
- [6] C. Bambi and K. Freese, Phys. Rev. D **79**, 043002 (2009), arXiv:0812.1328 [astro-ph].
- [7] D. J. Kaup, Phys. Rev. **172**, 1331 (1968).
- [8] S. L. Liebling and C. Palenzuela, Living Rev. Relativ. **15**, 6 (2012), arXiv:1202.5809 [gr-qc].
- [9] P. V. P. Cunha, J. A. Font, C. Herdeiro, E. Radu, N. Sanchis-Gual, and M. Zilhão, Phys. Rev. D **96**, 104040 (2017), arXiv:1709.06118.
- [10] H. Olivares, Z. Younsi, C. M. Fromm, M. De Laurentis, O. Porth, Y. Mizuno, H. Falcke, M. Kramer, and L. Rezzolla, Mon. Not. R. Astron. Soc. **497**, 521 (2020), arXiv:1809.08682 [gr-qc].